THE JOURNAL OF PHYSICAL CHEMISTRY C
A JOURNAL OF THE AMERICAN CHEMICAL SOCIETY

pubs.acs.org/JPCC

Article

Chemical Vapor Deposition of 2D Crystallized g-C_3N_4 Layered Films

Eugene B. Chubenko,* Nikolai G. Kovalchuk, Ivan V. Komissarov, and Victor E. Borisenko

Cite This: J. Phys. Chem. C 2022, 126, 4710−4714

Read Online

ACCESS | Metrics & More | Article Recommendations

ABSTRACT: We have developed a technology and for the first time, present here, the fabrication of continuous two-dimensionally crystallized g-C_3N_4 layered thin films oriented in a hexagonal lattice c-plane on glass and monocrystalline silicon substrates using chemical vapor deposition from a melamine source. Scanning electron microscopy and X-ray diffraction studies revealed that such films with a smooth surface and good crystalline quality as thick as up to 1.2 μm can be formed at a synthesis temperature of 550−625 °C. They are transparent in the visible range and demonstrate intense photoluminescence (PL) at room temperature. It was found that the band gap of the obtained material and its PL spectral range are shifting to the lower energies at high synthesis temperatures. Oriented g-C_3N_4 layered thin films deposited on flat solid substrates are promising for integrated electronics and optoelectronics.

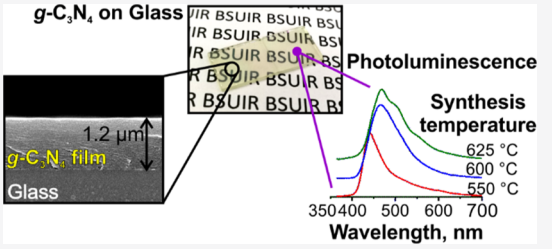

Downloaded via Eugene Chubenko on April 4, 2022 at 08:25:39 (UTC).
See https://pubs.acs.org/sharingguidelines for options on how to legitimately share published articles.

INTRODUCTION

Bright luminescence in the visible range and high photocatalytic efficiency of graphitic carbon nitride (g-C_3N_4), which is a wide band gap semiconductor (2.70−2.88 eV),[1,2] resulted in a great amount of research efforts on this material carried out by the global scientific community till date.[1−3] However, one can admit that electronic properties of the material and its application in electronics and optoelectronics remain notably out of the research scope. One of the reasons is that conventional synthesis of g-C_3N_4 employs thermal decomposition of precursors (melamine, urea, thiourea, cyanamide, and dicyanamide) followed by polymerization of the products in closed space crucibles.[2−8] The produced material has a form of a yellowish-white bulk crust usually consequently grinded down into a fine powder.[2,5] In that form, it is neither directly suitable for electronic nor optoelectronic devices. Thin films deposited on flat substrates are necessary for that applications.

There are several reports published on the deposition of g-C_3N_4 thin films on rigid and flexible substrates.[1,2,9−12] Some of them propose g-C_3N_4 particles produced by grinding or ultrasonic exfoliation from a presynthesized bulk material to mix with other semiconductors and/or polymers and then to deposit the mixture on a substrate surface. Such coatings are not uniform in the surface morphology and crystallinity. They are good for photocatalysis but not for electronics.

Another approach supposes substrates to be placed in a sealed crucible together with a precursor (melamine or mixture of melamine and urea/thiourea)[13−17] and annealed at a temperature sufficient for synthesis of g-C_3N_4. Both the precursor and the substrate are kept at the same temperature. Precursor vapors and reaction products fill the whole closed space of the crucible and then condensate on the substrate surface. Virgin or indium tin oxide-covered glasses, silica, silicon, or more exotic carbon cloth were used as substrates.[13−17] The deposited covers were just an array of g-C_3N_4 particles and sheets with limited crystallinity scattered on the substrate surface. It seems to be a result of overheating of the precursor and thus giving rise a vapor of molecular blocks randomly adsorbed at the surface of the substrates. There was an attempt to separate the heating zones for the precursors (300 °C) and substrates (550 °C).[18] Only ultrathin (10−150 nm) g-C_3N_4 films with poor crystallinity, as evident from the presented X-ray diffraction (XRD) data, were succeeded to be formed.

Independently, we developed and presented here two-zone chemical vapor deposition of g-C_3N_4 films distinguishing from that in ref 18 by (i) the increased temperature in the precursor evaporation zone to 350 °C in order to complete melamine → melam → melem → melon[5] transformation there; (ii) the use of dry argon instead of nitrogen, which is not chemically inert for evaporating compounds; and (iii) an extension of the substrate temperature to 625 °C. The above conditions modify the deposition peculiarities, providing formation of layered films with high crystalline quality in an order extended thickness range.

METHODS

Sodium silicate glass plates conventionally used for optical microscopy and standard antimony-doped (0.01 Ω·cm)

Received: December 15, 2021
Revised: February 15, 2022
Published: February 23, 2022

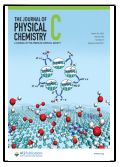

© 2022 American Chemical Society

https://doi.org/10.1021/acs.jpcc.1c10561
J. Phys. Chem. C 2022, 126, 4710−4714

monocrystalline silicon (100) wafers were used to cut 10 × 10 mm^2 substrates. The substrates were chemically cleaned before loading to the furnace.

The two-zone open tube furnace was used for chemical vapor deposition of the films (Figure 1). The inner diameter of the quartz tube was 14 mm. Before heating, an open ceramic crucible filled with 2 g of melamine powder was loaded into expected "low" temperature zone of the furnace. Glass and silicon substrates were horizontally placed into the expected "high"-temperature zone. Then, the furnace tube was filled with dried argon at a gas flow of 150 cm^3/min, which was maintained invariably during the whole deposition process. The "high"-temperature zone started heating first. As soon as its temperature reached a desired temperature in the range of 500−650 °C, the temperature in the "low"-temperature zone was increased to 350 °C. Both temperatures were maintained with an accuracy of ±5 °C.

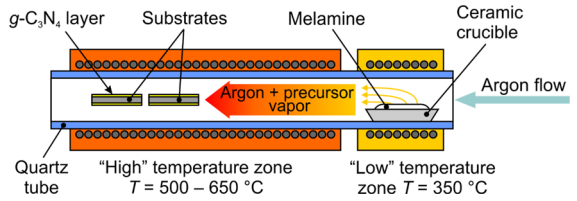

Figure 1. Schematic of the open tube two-zone furnace used for chemical vapor deposition of thin films from melamine.

Upon 50 min of stabilized temperatures in both zones, their heating was stopped leaving the furnace to cool under the argon flow. We noted that some amount of melamine was left in the crucible after the film deposition, thus indicating that this source was not exhausted, and the pressure of the melamine-produced vapor was constant within the whole high-temperature deposition cycle.

Morphology of the synthesized films was analyzed with scanning electron microscopy (SEM) using Hitachi S-4800 operating at an electron acceleration voltage of 15 kV. Atomic composition of the film material was studied with energy-dispersive X-ray (EDX) spectroscopy using a Bruker QUANTAX 200 EDX spectrometer. Crystalline phases in the films were identified by XRD analysis using a DRON-4 diffractometer using Cu Kα line (λ = 1.54184 Å). Photoluminescence (PL) spectra were recorded at room temperature with a SOLAR TII MS7504i spectrophotometer equipped with a Proscan HS101 CCD camera as a detector. A narrow monochromatic line of 345 nm wavelength (3.59 eV) cut by the double monochromator SOLAR TII DM 160 from the radiation of 1000 W xenon lamp was used to excite PL. Transmittance of the films on glass substrates was recorded at room temperature with a Proscan MC124 spectrophotometer. The refractive index of the films was measured with the ellipsometer using the light of 633 nm wavelength.

RESULTS AND DISCUSSION

All the films synthesized onto glass and silicon substrates were continuous and uniform with a rather smooth surface. SEM images in Figure 2 show that depending on the substrate temperature, the films have a slight wave-like morphology, originating from the substrate/film interface. Its "amplitude" increases from several nanometers after deposition at 550 °C to 100−200 nm in the sample fabricated at 625 °C. In spite of the "waves," the films have good adhesion to the substrates.

The thickness of the films estimated from the SEM images gets its maximum at the synthesis temperature of 600 °C, reaching 1.15 μm on glass and 0.90 μm on silicon (Figure 2). The layered structure of the films is well resolved. Thickness of an individual layer ranges from 18 to 37 nm. It is practically independent on the synthesis temperature and material of the substrate. We have experimentally noted that below 500 °C and above 650 °C, no films are formed, which is also inherent for a bulk g-C_3N_4 synthesis process.[5]

EDX analysis of the films reveled them to consist of nitrogen and carbon. The C_C/C_N ratio reduced from 0.67 for the 550 °C sample to 0.62 for the 625 °C sample. In all cases, it remains below 0.75 for stoichiometric g-C_3N_4, which evidences a carbon loss in the deposited carbon-containing species.[5,19]

XRD analysis showed good hexagonal crystallinity of the films synthesized on both amorphous glass and monocrystalline silicon substrates (Figure 3). The prominent line at 2θ = 27.65−27.80°, corresponding to the g-C_3N_4 (002) plane, has the highest intensity for the films deposited at 600 °C, which correlates with the film thickness reaching its maximum at that temperature. An absence of the diffraction peak at 2θ = 12−13° usually assigned to the (100) reflex typical for bulk and powdered g-C_3N_4 samples is pointing at a strong one-direction orientation of the crystallites in the films. Meanwhile, in the films synthesized at 600 °C on the glass substrate, an additional weak peak, corresponding to the (004) plane, in bulk g-C_3N_4 was detected.

The interplane distances d_{002} in the films calculated using (002) peak positions decrease with the synthesis temperature

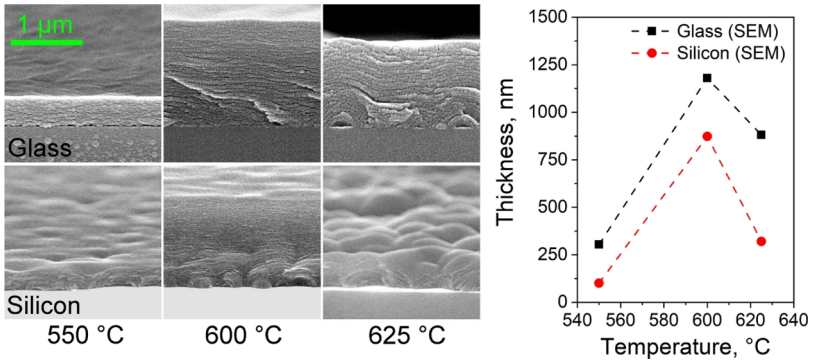

Figure 2. SEM images and thicknesses of the films synthesized on glass and silicon substrates at different temperatures. The 1 μm scale bar is applicable to all images.

https://doi.org/10.1021/acs.jpcc.1c10561
J. Phys. Chem. C 2022, 126, 4710−4714

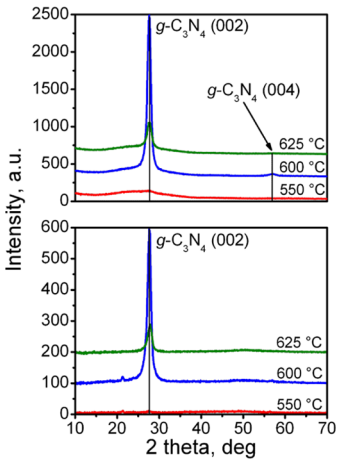

Glass

Synthesis temperature, °C	d_{002}, Å	Crystallite size, nm
550	3.247	38.4
600	3.224	75.4
625	3.224	35.7

Silicon

Synthesis temperature, °C	d_{002}, Å	Crystallite size, nm
550	3.252	42.9
600	3.207	69.4
625	3.224	35.9

Figure 3. XRD patterns from the g-C_3N_4 films synthesized at different temperatures on glass and silicon substrates and data extracted from them. The peaks are identified using ICDD database.

(Figure 3). They occur to be substantially smaller than that (3.40 Å) in a perfect g-C_3N_4 crystal with a tri-s-triazine structure.[20] The size of g-C_3N_4 crystallites calculated from the XRD data using the Scherrer equation varied with the synthesis temperature increasing from 550 to 600 °C up to 70−75 nm and then dropping down to 35−36 nm at 625 °C. These are two times bigger than the thickness of the distinctive layers visible at the SEM images.

The films are optically transparent in the visible range. Their transmittance recorded with the use of the samples on glass substrates is illustrated in Figure 4. The extracted optical band gap of the film material monotonously decreases with the synthesis temperature from 3.03 eV for 550 °C to 2.83 eV for 625 °C.

The film material demonstrates bright broad band PL in the visible range at room temperature. The spectra presented in Figure 5a show that the maximum of its intensity undergoes red shift with increasing synthesis temperature from 2.81 V to 2.65 eV. Broad and asymmetric character of the spectra indicates a number of excited charge carrier recombination

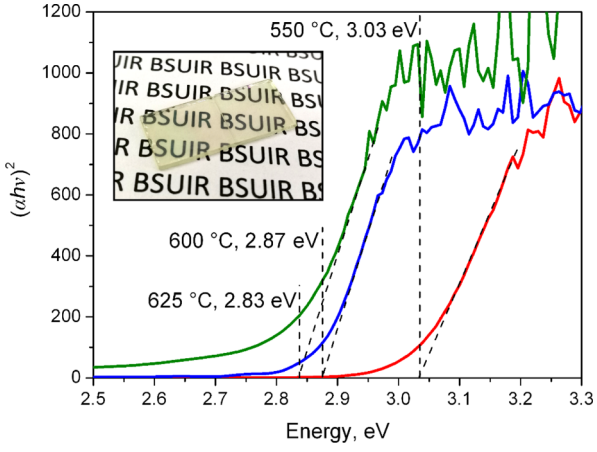

Figure 4. Tauc plots for the transmittance (α) of g-C_3N_4 films synthesized on glass substrates at different temperatures. Inset depicts an actual view of the sample fabricated at 600 °C, illustrating its transparency in the visible range. Absorption in the blue range defines its yellowish appearance.

processes contributing to the light emission. Recombination through specific energy levels in the material band gap schematically shown in Figure 5b looks dominant over conventional for semiconductors band-to-band recombination. The maximum absolute intensity of PL was reached in the samples fabricated at 600 °C on both glass and silicon substrates. PL intensity from the g-C_3N_4 films synthesized at 625 °C slightly decreases but remains higher than that from the samples obtained at 550 °C. Obviously, the PL intensity from the g-C_3N_4 films correlates with their thickness.

Luminescence of the synthesized thin films has much in common with that of bulk g-C_3N_4 synthesized from melamine.[21] The observed red shift of PL is caused by the change in the intensity ratios for the recombination processes involved (Figure 5b) in g-C_3N_4 synthesized at different temperatures. With an increase in the synthesis temperature, the role of radiative transitions with lower energies increases, which is a result of the changes in the material energy band structure. It is also responsible for the optical band gap narrowing detected by transmittance measurements. In fact, the band gap in g-C_3N_4 is the energy difference between its valance band formed by C−N σ-bonds with sp^3-hybridization and C−N π-bonds with sp^2-hybridization and conduction band, which is a superposition of excited σ^*- and π^*-bonds, as schematically presented in Figure 5b.[22,23] Degree of polymerization of g-C_3N_4 is known to increase with an increase in the polymerization temperature[22,23] because more and more tri-s-triazine units form chemical π-bonds with each other. Consequently, the energy band structure transforms from σ-bond-conjugated configuration (left part of the diagram in Figure 5b) to π-bond-conjugated one with lower energy transitions in the band gap (right part of the diagram in Figure 5b).

The refractive index of the films on silicon substrates examined by the ellipsometry technique shows that it changes from 1.139 for the sample fabricated at 550 °C to 2.316 at 600 °C and to 2.128 at 650 °C. These are comparable to those reported for bulk g-C_3N_4, ranging from 1.40 to 1.95.[24−26] In contrast to theoretical estimations and measurements performed on nonstoichiometric CN_x samples, we have directly evaluated experimentally the refraction index of g-C_3N_4 thin films composed of one direction-oriented crystallites.[24,25] The unexpected for the first look "fall down" of the refractive index in the 550 °C sample correlates with the variation of the optically extracted band gap and PL data for that temperature and other temperatures of synthesis.

Discussing the results obtained, it is worthwhile to note that possibilities to fabricate thin films of materials with hexagonal crystal lattices strongly oriented in the c [002] crystallographic direction on amorphous substrates were previously demonstrated for GaN, AlN, ZnO, and Bi_2Se_3.[27−30] Geometrical selection in the growth of the nucleated crystals when adatoms possess high kinetic energy is considered to be involved.[28] In our experiments, molecular blocks of hexagonally arranged atoms (preferably melon with a tri-s-triazine structure) are supposed to come to the substrate surface. Their energy is relatively low being defined by the thermal energy obtained during evaporation of the precursor. Thus, the "geometrical" scenario looks not realistic. Instead, the dominant c-oriented growth of g-C_3N_4 crystal layers forming the films is most probably controlled by two facts: (i) the large difference in energy between strong covalent atomic interaction in-plane (a-direction [210]) and weak perpendicular-to-plane van der

https://doi.org/10.1021/acs.jpcc.1c10561
J. Phys. Chem. C 2022, 126, 4710−4714

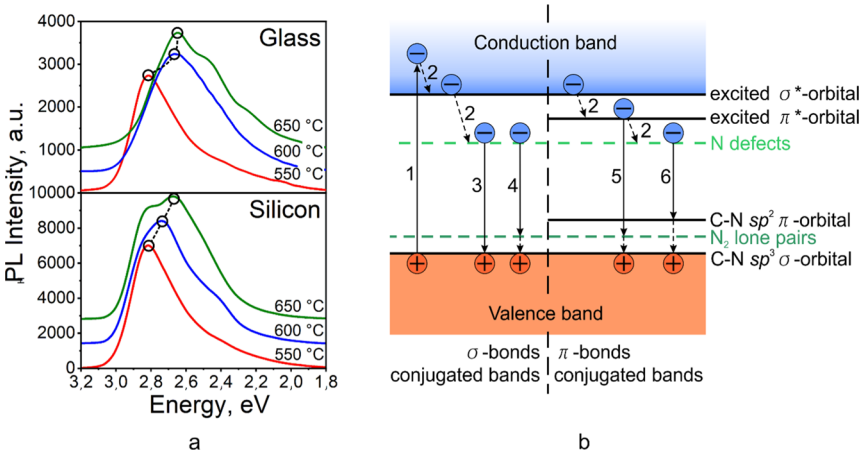

Figure 5. Normalized spectra of PL from the g-C_3N_4 films synthesized at different temperatures on glass and silicon substrates (a) and possible recombination mechanisms of light excited electrons in this material (b): 1—optical excitation of electrons, 2—nonradiative electron energy relaxation, 3—nitrogen defect level to valence band radiative transition, 4—nitrogen defect level to nitrogen lone pair level radiative transition, 5—conduction band in π-bond-conjugated system to nitrogen lone pair level radiative transition, and 6—nitrogen defect level to valence band in π-bond-conjugated system radiative transition.

Waals interaction (c-direction [002]) in g-C_3N_4 crystals and (ii) the difference in the surface energy for c-and a-oriented crystallites. As a result, tri-s-triazine building units arrived onto the substrate surface polymerize there by stacking in-plane with each other. Upon two-dimensional (2D) completion of the monomolecular layer, an upper one starts to be formed. Thus, layer-by-layer growth of g-C_3N_4 films is believed to take place. It is supported by the strong XRD peak, indicating only perfect (002) planes of g-C_3N_4 in the synthesized films.

Kinetics of the polymerization process is obviously different for the synthesis temperatures used. In all cases, argon carrier gas flow and substrate positions along the furnace tube remain constant. However, the chemical transformations of evaporated melamine to tri-s-triazine building units do not happen instantly and take some time. The polymerization rate is temperature dependent. It means that at different synthesis temperatures, the amount of polymerized tri-s-triazine units transported to the substrates should also be different. The maximum concentration of these units at the substrate surface is supposed to be achieved at 600 °C. At the higher synthesis temperature of 625 °C, the decomposition became more intensive,[5,19] and tri-s-triazine molecules could disintegrate before they reach the substrate surface. At a lower synthesis temperature, the polymerization of these molecules is evidently not complete. As a result of the competition between polymerization and decomposition processes, the thickest g-C_3N_4 film was synthesized at 600 °C.

An increase in the number of the synthesized molecular layers brings mechanical stresses, stimulating formation of interlayer interfaces where they can relax, possibly with an assistance of point defects (vacancies, nitrogen interstitials, and oxygen atoms) pushed there. The observed reduced interplane distances d_{002} could be an indication of that.

The origin of the wave-like morphology is considered to be associated with two main factors. The first is defects at the substrate surface and crystal lattice mismatch, affecting nucleation and growth kinetics. The SEM images revealed an increased number of defects at the g-C_3N_4/substrate interfaces for the crystalline silicon substrates as compared to the amorphous glass ones. Orientation effects from the crystalline substrate and related stresses in the film are considered to be more pronounced in the case of monocrystalline silicon. It is also supported by the observed difference in the PL and optical properties of the films fabricated on silicon and glass substrates. The second could be a difference in the thermal expansion coefficients and surface energies of the substrate material and g-C_3N_4 and thus giving rise mechanical stresses relaxing by the formation of the wave-like surface of the films. The regularity of the "waves" and an increase in their "amplitude" with temperature is in line with the last hypothesis.

CONCLUSIONS

We have demonstrated for the first time that chemical vapor deposition can be successfully employed for a controlled fabrication of continuous g-C_3N_4 thin films with thicknesses up to 1.2 μm on glass and silicon substrates using melamine as a vapor source. The films have a unique layered structure with a strong one c-axis orientation of 2D crystallites in each layer. The film thickness and its morphology are dependent on the synthesis temperature, while the temperature used for evaporation of the precursor and total time of the deposition process should also be considered for their control. The measured structure, optical transmittance, and luminescent properties of the films demonstrate them to be promising for integrated optoelectronic and nanoelectronic applications. Both, an attempt to fabricate g-C_3N_4 thin films by molecular beam epitaxy using an organic precursor and a study of charge carrier transport in such films could be useful for that.

AUTHOR INFORMATION

Corresponding Author

Eugene B. Chubenko − *Department of Micro- and Nanoelectronics, Belarusian State University of Informatics and Radioelectronics, Minsk 220013, Belarus;* orcid.org/0000-0002-1818-523X; Email: eugene.chubenko@gmail.com

Authors

Nikolai G. Kovalchuk − *Department of Micro- and Nanoelectronics, Belarusian State University of Informatics and Radioelectronics, Minsk 220013, Belarus*

https://doi.org/10.1021/acs.jpcc.1c10561
J. Phys. Chem. C 2022, 126, 4710−4714

Ivan V. Komissarov − *Department of Micro- and Nanoelectronics, Belarusian State University of Informatics and Radioelectronics, Minsk 220013, Belarus*

Victor E. Borisenko − *Department of Micro- and Nanoelectronics, Belarusian State University of Informatics and Radioelectronics, Minsk 220013, Belarus*

Complete contact information is available at: https://pubs.acs.org/10.1021/acs.jpcc.1c10561

Notes

The authors declare no competing financial interest.

■ ACKNOWLEDGMENTS

The authors are grateful to D. V. Zhigulin for the SEM and EDX analyses and to Professor V. V. Uglov for XRD analysis of the samples. The authors declare no conflicts of interest. This research was funded by the Ministry of Education of the Republic of Belarus, Project 1.4 of the Belarus State Research Program "Material science, novel materials and technologies."

■ REFERENCES

(1) Wen, J.; Xie, J.; Chen, X.; Li, X. A Review on g-C_3N_4-based Photocatalysts. *Appl. Surf. Sci.* **2017**, *391*, 72−123.

(2) Wang, A.; Wang, C.; Fu, L.; Wong-Ng, W.; Lan, Y. Recent Advances of Graphitic Carbon Nitride-Based Structures and Applications in Catalyst, Sensing, Imaging, and LEDs. *Nano-Micro Lett.* **2017**, *9*, 47.

(3) Wang, Y.; Liu, L.; Ma, T.; Zhang, Y.; Huang, H. 2D Graphitic Carbon Nitride for Energy Conversion and Storage. *Adv. Funct. Mater.* **2021**, *31*, 2102540.

(4) Sudhaik, A.; Raizada, P.; Shandilya, P.; Jeong, D.-Y.; Lim, J.-H.; Singh, P. Review on Fabrication of Graphitic Carbon Nitride Based Efficient Nanocomposites for Photodegradation of Aqueous Phase Organic Pollutants. *J. Ind. Eng. Chem.* **2018**, *67*, 28−51.

(5) Thomas, A.; Fischer, A.; Goettmann, F.; Antonietti, M.; Müller, J.-O.; Schlögl, R.; Carlsson, J. M. Graphitic Carbon Nitride Materials: Variation of Structure and Morphology and Their Use as Metal-Free Catalysts. *J. Mater. Chem.* **2008**, *18*, 4893−4908.

(6) Chubenko, E. B.; Denisov, N. M.; Baglov, A. V.; Bondarenko, V. P.; Uglov, V. V.; Borisenko, V. E. Recovery Behaviour of the Luminescence Peak From Graphitic Carbon Nitride as a Function of the Synthesis Temperature. *Cryst. Res. Technol.* **2020**, *55*, 1900163.

(7) Baglov, A. V.; Chubenko, E. B.; Hnitsko, A. A.; Borisenko, V. E.; Malashevich, A. A.; Uglov, V. V. Structural and Photoluminescence Properties of Graphite-Like Carbon Nitride. *Semiconductors* **2020**, *54*, 228−232.

(8) Denisov, N. M.; Chubenko, E. B.; Bondarenko, V. P.; Borisenko, V. E. Synthesis of Oxygen-Doped Graphitic Carbon Nitride From Thiourea. *Tech. Phys. Lett.* **2019**, *45*, 108−110.

(9) Safaei, J.; Mohamed, N. A.; Noh, M. F. M.; Soh, M. F.; Riza, M. A.; Mustakim, N. S. M.; Ludin, N. A.; Ibrahim, M. A.; Isahak, W. N. R. W.; Teridi, M. A. M. Facile Fabrication of Graphitic Carbon Nitride (g-C_3N_4) Thin Film. *J. Alloys Compd.* **2018**, *769*, 130−135.

(10) Bayan, S.; Gogurla, N.; Midya, A.; Ray, S. K. White Light Emission Characteristics of Two Dimensional Graphitic Carbon Nitride and ZnO Nanorod Hybrid Heterojunctions. *Carbon* **2016**, *108*, 335−342.

(11) Chetia, T. R.; Ansari, M. S.; Qureshi, M. Graphitic Carbon Nitride as a Photovoltaic Booster in Quantum Dot Sensitized Solar Cells: A Synergistic Approach for Enhanced Charge Separation and Injection. *J. Mater. Chem. A* **2016**, *4*, 5528−5541.

(12) Hu, C.; Chen, F.; Wang, Y.; Tian, N.; Ma, T.; Zhang, Y.; Huang, H. Exceptional Cocatalyst-Free Photo-Enhanced Piezocatalytic Hydrogen Evolution of Carbon Nitride Nanosheets from Strong In-Plane Polarization. *Adv. Mater.* **2021**, *33*, 2101751.

(13) Ye, L.; Wang, D.; Chen, S. Fabrication and Enhanced Photoelectrochemical Performance of MoS_2/S-doped g-C_3N_4Heterojunction Film. *ACS Appl. Mater. Interfaces* **2016**, *8*, 5280−5289.

(14) Guo, W.; Ming, S.; Chen, Z.; Bi, J.; Ma, Y.; Wang, J.; Li, T. A Novel CVD Growth of g-C_3N_4Ultrathin Film on NiC-o_2O_4Nanoneedles/Carbon Cloth as Integrated Electrodes for Supercapacitors. *ChemElectroChem* **2018**, *5*, 3383−3390.

(15) Bian, J.; Li, Q.; Huang, C.; Li, J.; Guo, Y.; Zaw, M.; Zhang, R.-Q. Thermal Vapor Condensation of Uniform Graphitic Carbon Nitride Films with Remarkable Photocurrent Density for Photoelectrochemical Applications. *Nano Energy* **2015**, *15*, 353−361.

(16) Ye, L.; Chen, S. Fabrication and High Visible-Light-Driven Photocurrent Response of g-C_3N_4Film: The Role of Thiourea. *Appl. Surf. Sci.* **2016**, *389*, 1076−1083.

(17) Jia, F.; Zhang, Y.; Hu, W.; Lv, M.; Jia, C.; Liu, J. In-situ Construction of Superhydrophilicg-C_3N_4Film by Vapor-Assisted Confined Deposition for Photocatalysis. *Front. Mater.* **2018**, *6*, 52.

(18) Chen, L.; Yan, R.; Oschatz, M.; Jiang, L.; Antonietti, M.; Xiao, K. Ultrathin 2D Graphitic Carbon Nitride on Metal Films: Underpotential Sodium Deposition in Adlayers for Sodium-Ion Batteries. *Angew. Chem., Int. Ed.* **2020**, *59*, 9067−9073.

(19) Jürgens, B.; Irran, E.; Senker, J.; Kroll, P.; Müller, H.; Schnick, W. Melem (2,5,8-triamino-tri-s-triazine), an Important Intermediate During Condensation of Melamine Rings to Graphitic Carbon Nitride: Synthesis, Structure Determination by X-ray Powder Diffractometry, Solid-State NMR, and Theoretical Studies. *J. Am. Chem. Soc.* **2003**, *125*, 10288−10300.

(20) Bojdys, M. J.; Müller, J.-O.; Antonietti, M.; Thomas, A. Ionothermal Synthesis of Crystalline, Condensed, Graphitic Carbon Nitride. *Chem.—Eur. J.* **2008**, *14*, 8177−8182.

(21) Chubenko, E. B.; Baglov, A. V.; Leonenya, M. S.; Yablonskii, G. P.; Borisenko, V. E. Structure of Photoluminescence Spectra of Oxygen-Doped Graphitic Carbon Nitride. *J. Appl. Spectrosc.* **2020**, *87*, 9−14.

(22) Choudhury, B.; Paul, K. K.; Sanyal, D.; Hazarika, A.; Giri, P. K. Evolution of Nitrogen-Related Defects in Graphitic Carbon Nitride Nanosheets Probed by Positron Annihilation and Photoluminescence Spectroscopy. *J. Phys. Chem. C* **2018**, *122*, 9209−9219.

(23) Zhang, Y.; Pan, Q.; Chai, G.; Liang, M.; Dong, G.; Zhang, Q.; Qiu, J. Synthesis and Luminescence Mechanism of Multicolor-Emitting g-C_3N_4Nanopowdersby Low Temperature Thermal Condensation of Melamine. *Sci. Rep.* **2013**, *3*, 1943.

(24) Reshak, A. H.; Khan, S. A.; Auluck, S. Linear and Nonlinear Optical Properties for AA and AB Stacking of Carbon Nitride Polymorph (C_3N_4). *RSC Adv.* **2014**, *4*, 11967−11974.

(25) Balaceanu, M.; Grigore, E.; Pavelescu, G.; Ionescu, F.; Roger, J. P. Optical Characteristics of Carbon Nitride Films Prepared by Hollow Cathode Discharge. *J. Optoelectron. Adv. Mater.* **2000**, *2*, 351−355.

(26) Jia, R.; Amulele, G.; Zinin, P. V.; Odake, S.; Eng, P.; Khabashesku, V.; Mao, W. L.; Ming, L. C. Elastic and Inelastic Behavior of Graphitic C_3N_4Under High Pressure. *Chem. Phys. Lett.* **2013**, *575*, 67−70.

(27) Matsuoka, T. Current Status of GaN and Related Compounds as Wide-Gap Semiconductors. *J. Cryst. Growth* **1992**, *124*, 433−438.

(28) Kao, H. L.; Shih, P. J.; Lai, C.-H. The Study of Preferred Orientation Growth of Aluminum Nitride Thin Films on Ceramic and Glass Substrates. *Jpn. J. Appl. Phys.* **1999**, *38*, 1526−1529.

(29) Detchprohm, T.; Hiramatsu, K.; Amano, H.; Akasaki, I. Hydride Vapor Phase Epitaxial Growth of a High Quality GaN Film Using a ZnO Buffer Layer. *Appl. Phys. Lett.* **1992**, *61*, 2688−2690.

(30) Jerng, S.-K.; Joo, K.; Kim, Y.; Yoon, S.-M.; Lee, J. H.; Kim, M.; Kim, J. S.; Yoon, E.; Chuna, S.-H.; Chun, Y. S. Ordered Growth of Topological Insulator Bi_2Se_3 Thin Films on Dielectric Amorphous SiO_2 by MBE. *Nanoscale* **2013**, *5*, 10618−10622.